

**Correlation between Stress Relaxation Dynamics and Thermochemistry for Covalent Adaptive Networks Polymer**

Journal:	<i>Materials Chemistry Frontiers</i>
Manuscript ID	QM-RES-06-2016-000094.R1
Article Type:	Research Article
Date Submitted by the Author:	03-Aug-2016
Complete List of Authors:	Kuang, Xiao; Institute of Chemistry, Chinese Academy of Sciences Liu, Guoming; Institute of Chemistry, Chinese Academy of Sciences, Dong, Xia; Institute of Chemistry, Chinese Academy of Sciences, CAS Key Lab. of Engineering Plastic Wang, Dujin; Institute of Chemistry, Chinese Academy of Sciences, State Key Laboratory of Polymer Physics and Chemistry



Journal Name

ARTICLE

## Correlation between Stress Relaxation Dynamics and Thermochemistry for Covalent Adaptive Networks Polymer

Xiao Kuang,<sup>a,b</sup> Guoming Liu,<sup>a</sup> Xia Dong,<sup>a</sup> Dujin Wang<sup>a,b\*</sup>Received 00th January 20xx,  
Accepted 00th January 20xx

DOI: 10.1039/x0xx00000x

www.rsc.org/

The smart polymers based on covalent adaptive networks (CANs) with reversible covalent bonds have drawn tremendous attention in the past few years. The relaxation properties of CANs polymers play an important role in their stimuli responsive capability. Here, we elucidate the correlation between the stress relaxation dynamics and reaction thermochemistry for CANs polymers. The Diels-Alder (DA) reaction based cross-linked elastomers are utilized as model CANs polymers. In-situ FTIR data reveals the dynamic reaction kinetics and thermodynamics at solid state. The influence of cross-linking density on the temperature-dependent stress relaxation time of the CANs polymers well above the gel point can be normalized by the relative distance to gel point conversion. Combining the Semenov-Rubinstein theory and Arrhenius' law, a simple scaling relationship between normalized relaxation time and reaction kinetics is established for CANs polymers.

### 1 Introduction

Covalent adaptive networks (CANs) polymers refer to the networks containing sufficient reversible cross-links.<sup>1-3</sup> CANs polymers combine the desirable attributes of conventional thermosets with the capability of responding to selective stimuli. A variety of smart polymers, such as self-healing,<sup>4-11</sup> shape memory<sup>12-18</sup> and recyclable thermosets<sup>19-24</sup> have been developed based on CANs polymers. On basis of network rearrangement mechanism and dynamic reactions, the CANs are grouped into two categories: reversible addition/condensation reactions and reversible exchange reactions. The bond exchange reactions, such as transesterification, follow a simultaneous bond-forming and bond-breaking process without a decrease in cross-linking density during the transition. However, the network rearrangement of reversible addition reaction, such as Diels-Alder (DA) reaction, follows bond-breaking, bond-forming reaction sequence. For example, increasing the temperature favours the endothermic retro Diels-Alder (rDA) reaction and the reaction shifts toward the reactants, thereby decreasing the amount of adducts and the cross-links.<sup>25-29</sup>

It is well known that time-temperature superposition (TTS) principle is a powerful tool for understanding the temperature-dependent mechanical properties for polymers. In regard to the dynamic polymers, TTS has been used with success on materials when bond dynamics and conversion are not strong functions of

temperature.<sup>30-32</sup> The relaxation properties of CANs based on reversible exchange bond, such as transesterification, have been extensively studied.<sup>33-37</sup> The temperature-dependent relaxation dynamics were revealed by Arrhenius' law. The network rearrangement and relaxation for transesterification type CANs are dominated by reaction kinetics, and their temperature-dependent relaxation properties are described by TTS.<sup>34</sup> In DA-type CANs, however, both the reaction kinetics and cross-linking density are influenced by temperature. The superposition concept is inappropriate for such CANs with temperature-dependent equilibrium chemical structures.<sup>28</sup> Moreover, the influence of network structure, such as cross-linking density, on the relaxation properties has not been well understood in CANs polymers yet. Therefore, deeper insight into relaxation behaviour for CANs polymers at molecular scale is urgently needed.

Recently, the direct relationship between the bond lifetime and the relaxation behaviour for associating polymers (such as amphiphilic systems and ionomers) was obtained by applying the Semenov-Rubinstein (SR) model.<sup>38-40</sup> This model also provides an appropriate description of the linear dynamics for DA network near the gel point.<sup>41</sup> The maximum relaxation time ( $\tau_{\max}$ ) of the associating network with many reversible stickers corresponds to the rheological lifetime of the cluster ( $\tau_1$ ) (eq. 1), which is proportional to the bond lifetime  $\tau_b$  and the relative distance to the Flory gel point in conversion ( $\epsilon$ ) (eq. 2).

$$\tau_{\max} = \tau_1 \cong C\tau_b\epsilon \quad (1)$$

$$\epsilon = \frac{p - p_{\text{gel}}}{p_{\text{gel}}} \quad (2)$$

$$p_{\text{gel}} = 1 / \sqrt{r(1 - f_M)(1 - f_F)} \quad (3)$$

where  $\tau_b$  equals to the inverse of reverse reaction kinetic rate constant ( $k_r$ ). In eq.2,  $p$  is the conversion of the limiting reagent or

<sup>a</sup> Beijing National Laboratory for Molecular Sciences, CAS Key Laboratory of Engineering Plastics, Institute of Chemistry, Chinese Academy of Sciences, Beijing, 100190, China. E-mail: djwang@iccas.ac.cn; Fax: +86-10-82618533; Tel: +86-10-82618533

<sup>b</sup> University of Chinese Academy of Sciences, Beijing 100049, China.

† Electronic Supplementary Information (ESI) available: [Experimental procedures; NMR, FTIR, and stress relaxation graphics]. See DOI:10.1039/x0xx00000x.

the fraction of associated stickers (such as DA adduct), and  $p_{gel}$  is the gel point conversion between maleimide and furan monomers.

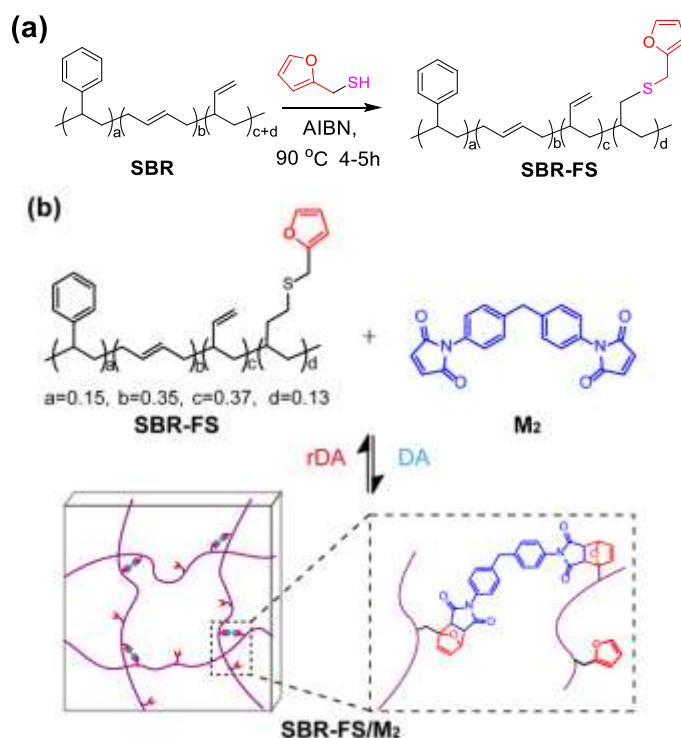
The prediction of  $p_{gel}$  is described by the Flory-Stockmayer equation.<sup>42</sup> In eq. 3,  $r$  is the stoichiometric ratio of maleimide to furan moieties ( $r \leq 1$ );  $f_M$  and  $f_F$  are the degree of functionality for the maleimide and furan monomers, respectively. The dynamic polymers well above gel point conversion, i.e.  $\epsilon \gg 0$ , are not further discussed by SR theory. Such CANs polymers with long relaxation time are hard to measure by conventional dynamic rheological test. Whether SR theory can be applied to CANs polymers well above gel point still remains unknown.

In this study, we aim to elucidate the correlation between the relaxation dynamics and reaction thermochemistry for CANs polymers well above gel point. Specifically, the influences of temperature and cross-linking density on the stress relaxation time of DA-type CANs elastomers were investigated. The *in-situ* FTIR was utilized to measure the reaction kinetics and thermodynamics at solid state. The tensile stress relaxation tests were conducted to evaluate the relaxation properties of DA-type CANs polymers with different cross-linking densities. We took advantage of Arrhenius' law and Semenov-Rubinstein theory to analyse the temperature-dependent stress relaxation time of CANs polymers and demonstrated the relaxation mechanism at molecular scale.

## 2 Results and discussion

### 2.1 Modification and cross-linking of SBR

The SBR with reactive vinyl double bonds was modified by furfuryl mercaptan through thermal initiated thiol-ene addition.<sup>25</sup>



**Scheme 1.** (a) Modification of SBR with furfuryl mercaptan by thiol-ene addition. (b) Synthesis of Diels-Alder type CANs polymers (SBR-FS/M<sub>2</sub>).

The furfuryl functional SBR (SBR-FS) was characterized by <sup>1</sup>H NMR analysis. As shown in Fig. S1, ESI+ the peaks at  $\delta = 7.34, 6.29,$  and  $6.16$  ppm are ascribed to the protons of the furan ring attached on the polymer chain. The peak at  $\delta = 3.68$  ppm is attributed to the methylene protons of furfuryl. Degree of furan substitution ( $DS$ ) was calculated to be 13.2% by eq. S1. The <sup>13</sup>C NMR spectrum also confirms the successful modification of SBR with corresponding peaks of furfuryl group (Fig. S2, ESI+). From GPC results, the molecular weight distribution of SBR-FS is very narrow, suggesting the negligible cross-linking reaction during the modification (Table S1). In addition, the average functionality of the furfuryl functional SBR was evaluated to be 116~119.

The chemical modification was further followed by FTIR spectrum. As shown in Fig. 1a, the appearance of the furan ring COC bands ( $\nu^{as}_{COC} = 1071 \text{ cm}^{-1}$ , and  $\nu^s_{COC} = 1009 \text{ cm}^{-1}$ ), the C=C stretching vibration of the furan ring ( $\nu^s_{CC} = 1505 \text{ cm}^{-1}$ ), the CH in-plane deformation of furan ( $\delta^{ip}_{CH} = 1150 \text{ cm}^{-1}$ ), and the CH out-of-plane deformation vibration of furan ( $\delta^{op}_{CH} = 731 \text{ cm}^{-1}$ ) clearly indicate the presence of furan groups on the polymer chain after modification.<sup>43</sup> Moreover, the decrease of the vinyl C=C stretching vibration ( $\nu^s_{CC} = 1639 \text{ cm}^{-1}$ ) intensity confirms the grafting of furan group to the chain of SBR via thiol-ene reaction.<sup>44</sup>

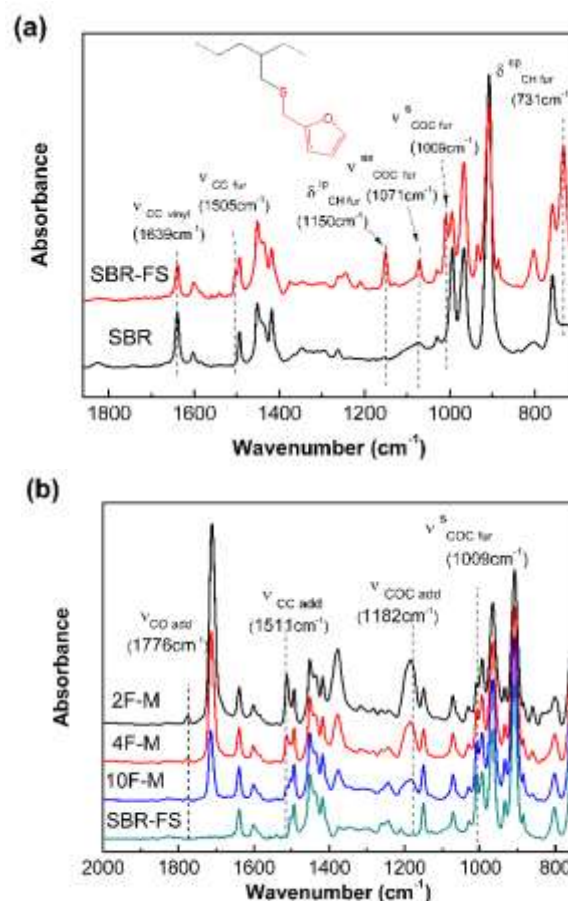


**Fig. 1** FTIR absorption spectra of (a) pristine SBR and SBR-FS samples, (b) SBR-FS and cross-linked rubbers with different furan/maleimide ratios.

The cross-linked samples with different furan/maleimide molar ratios ( $F/M = x/1$ ,  $x=2, 4$  and  $10$ ) are denoted as  $xF-M$ . The cross-linking reaction between SBR-FS and bismaleimide ( $M_2$ ) cross-linker was also characterized by FTIR spectra. As shown in Fig. 1b, the formation of the DA adduct is evidenced by the appearance of adduct bands ( $\nu_{COC} = 1182 \text{ cm}^{-1}$ ,  $\nu_{CNC} = 1194 \text{ cm}^{-1}$ ,  $\nu_{CO} = 1777 \text{ cm}^{-1}$ ), and furan C=C stretching ( $\nu_{CC} = 1511 \text{ cm}^{-1}$ ) in all the cross-linked polymers with different furan/maleimide ( $F/M$ ) ratios.<sup>45-46</sup> The samples with lower  $F/M$  ratios (higher cross-linker content) show stronger bands intensity. Meanwhile, the amount of furan moieties, as indicated by the band of  $1009 \text{ cm}^{-1}$  ( $\nu_{COC}^s$ ), decreases with increasing amount of  $M_2$  cross-linking agent. The equilibrium controlled DA reaction is not complete for stoichiometric ratio of  $F/M$  moieties ( $F/M=1$ ).<sup>47</sup> With sufficient furan moieties ( $F/M>1$ ), however, nearly complete conversion of maleimide was achieved as indicated by the absence of maleimide characteristic band ( $\delta_{CC} = 827 \text{ cm}^{-1}$ ).

The DA reaction between the furan moieties in modified polymer chains and the maleimide moieties in the cross-linker produces a thermally reversible network. Solubility tests were used to determine the cross-linking and de-cross-linking effects of the reversible network. The initial reaction mixture solution (Fig. 2a) changed into gel quickly after treating at mild temperature ( $70 \text{ }^\circ\text{C}$ ) (Fig. 2b). Upon heating to  $140 \text{ }^\circ\text{C}$ , the resulting polymer gel was completely reversed to clear and fluid solution (Fig. 2c). Annealing the above solution at  $70 \text{ }^\circ\text{C}$  led to gel formation again (Fig. 2d). The heat induced sol-gel transition results from the reversible DA/rDA reactions, which was depicted by FTIR in solid state.

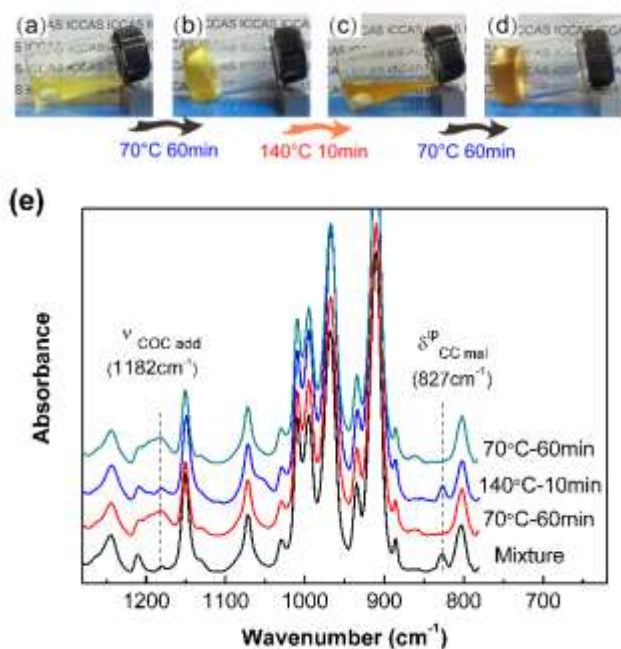


**Fig. 2** The sol-gel transition process of 4F-M sample in dichlorobenzene solvent when temperature changed: (a) initial reaction mixture, (b) gel formation at  $70 \text{ }^\circ\text{C}$  after 1 hr, (c) back to soluble solution in 10 min at  $140 \text{ }^\circ\text{C}$ , (d) gel reformation at  $70 \text{ }^\circ\text{C}$

after 1 hr. (e) FTIR spectra of 10F-M mixture under different thermal treatments.

The 10F-M sample was subjected to repeated DA ( $70 \text{ }^\circ\text{C}$ )-rDA ( $140 \text{ }^\circ\text{C}$ )-DA( $70 \text{ }^\circ\text{C}$ ) reactions cycles and tested by FTIR (Fig. 2e). In the original reactive mixture, the presence of free unreacted maleimide was reflected by the C=C deformation of maleimide at  $827 \text{ cm}^{-1}$ . The maleimide signal nearly disappeared after treating at  $70 \text{ }^\circ\text{C}$  for 1 hr via DA reaction, accompanied with the appearance of adduct signal at  $1182 \text{ cm}^{-1}$ . When the sample was treated at  $140 \text{ }^\circ\text{C}$ , the band of  $827 \text{ cm}^{-1}$  nearly recovered its initial value and the band of  $1182 \text{ cm}^{-1}$  decreased obviously via rDA reaction. Thus, both of these two bands can be utilized to evaluate the DA/rDA reaction.

## 2.2 Thermal analysis

The DSC method offers useful insights in characterizing materials with thermally responsive properties. The DSC heating curves of all the CANs polymers show a glass transition and a broad endothermic process attributed to rDA reaction (Fig. 3a). The glass transition temperature ( $T_g$ ) ranging from  $-12$  to  $0 \text{ }^\circ\text{C}$ , increases with the amount of cross-linker. The rDA reaction with peak temperature ( $T_{rDA}$ ) locates at  $119 \text{ }^\circ\text{C}$  for all the sample. The reaction enthalpy ( $\Delta H_{rDA}$ ) increases with the  $M_2$  content indicating increasing amount of DA adducts. It should be noted that the rDA reaction of endo and exo stereoisomers connected to aromatic structures take places at close temperatures, which are hard to separate by DSC.<sup>48</sup>

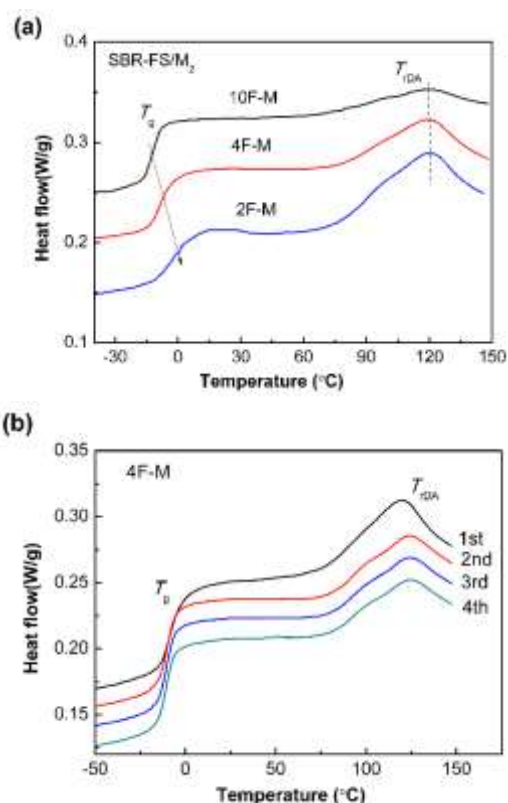


**Fig. 3** (a) DSC heating curves for CANs polymers with different furan/maleimide ratios. (b) Four repeated DSC heating traces of 4F-M samples. The scan rate was  $10 \text{ }^\circ\text{C min}^{-1}$ .

Sample	$T_g$ (°C)	$T_{rDA}$ (°C) (1 <sup>st</sup> )	$\Delta H_{rDA}$ (J g <sup>-1</sup> ) (1 <sup>st</sup> )	$T_{rDA}$ (°C) (2 <sup>nd</sup> )	$\Delta H_{rDA}$ (J g <sup>-1</sup> ) (2 <sup>nd</sup> )
10F-M	-11.8	118.9	3.20	122.6	2.96
4F-M	-6.9	119.1	9.39	122.3	5.88
2F-M	-0.4	118.3	11.52	121.8	9.73

**Table 1** Thermal properties of CANs elastomers measured by DSC

As shown in Fig. 3b, the rDA reaction enthalpy decreases in the second heating run. It means that DA adduct formation is incomplete in the short duration of cooling process. The repeated thermal cycles show comparable peak areas and no obvious peak shift indicating excellent thermal reversibility of the investigated systems. The thermal properties of the DA type CANs elastomers in cyclic tests are summarized in Table 1.

### 2.3 Dynamic mechanical thermal analysis

The thermal mechanical properties of the CANs elastomers were tested by DMTA in tensile mode. As shown in Fig. 4a, an obvious rubber plateau was observed in CANs elastomer after glass transition. The rubber plateau modulus enhances with increasing cross-linker content. However, the storage modulus starts to drop over 100 °C as a result of de-cross-linking via the rDA reaction. The single glass transition becomes broader with higher  $M_2$  content (Fig. 4b).

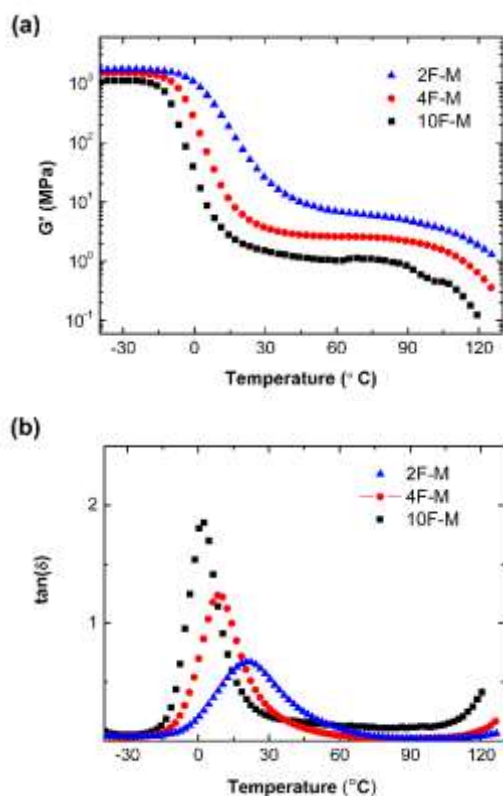


**Fig. 4** (a) Storage modulus ( $G'$ ) and (b)  $\tan \delta$  as a function of temperature for CANs polymers with different cross-linking densities.

**Table 2** Thermal mechanical properties of CANs elastomers

Sample	$\nu$ (mol m <sup>-3</sup> )	$M_c^a$ (g mol <sup>-1</sup> )	$\nu^b$ (mol m <sup>-3</sup> )	$T_g$ (°C)
10F-M	130	7155	159	1.9
4F-M	317	2937	398	8.9
2F-M	701	1326	844	20.7

measured by DMTA

<sup>a</sup> Calculated by  $M_c = \rho/\nu$ ,  $\rho$  is the density of rubber; <sup>b</sup> calculated by chemical analysis of the maleimide moieties.

The cross-linking density ( $\nu$ ) was evaluated from rubber theory by the following equation (eq. 4)<sup>49</sup>:

$$\nu = \frac{E}{2(1+\nu)RT} \quad (4)$$

where  $E$  is tensile modulus as measured by DMTA at 60°C from the rubbery plateau zone,  $\nu$  is the Poisson's ratio (0.5 for rubbers),  $R$  is the gas constant, and  $T$  is the absolute temperature.

The calculated apparent cross-linking densities ranging from 130~701 mol m<sup>-3</sup> increase with the cross-linker content for CANs elastomers (Table 2). These values are comparable to DA adduct densities determined by chemical analysis. This result suggests that the cross-links are uniformly distributed throughout the material. The small discrepancy between the calculated values and experimental results is not surprising. For one, the CANs polymers cross-linked by  $M_2$  cross-linker is not an ideal network. For another, the maleimide conversion was not 100 % at the reference temperature (60 °C) leading to the decrease of cross-linking density. The molecular weight of polymer chain between cross-linkers,  $M_c$ , was also obtained from the experimental cross-linking density.

### 3.4 Thermochemistry

By means of *in-situ* FTIR spectra, the characteristic peaks of maleimide at 827 cm<sup>-1</sup> (C=C deformation) and the adduct at 1182 cm<sup>-1</sup> (C-O-C stretching) were utilized to evaluate the DA/rDA reactions. Maleimide or adduct conversion ( $p$ ) were calculated by the following equation:

$$p = \frac{I_{100\%} - I}{I_{100\%} - I_0} \quad (5)$$

where  $I$  is the peak intensities of 827cm<sup>-1</sup> band (C=C deformation in maleimide) or 1182 cm<sup>-1</sup> band (C-O-C stretch in adduct) at the measurement temperature or time;  $I_{100\%}$  and  $I_0$  represent the corresponding peak intensities of 100 % and 0 of maleimide or adduct contents, respectively.

Comparable DA/rDA reaction conversion can be derived by eq. 5 using these two characteristic bands (Fig. S3, ES†). For simplicity, the reaction conversion was evaluated from the band of 827 cm<sup>-1</sup>, which doesn't overlap with other bands. When testing the samples

at elevated temperatures, it's better to use the band of  $1182\text{ cm}^{-1}$  to calculate the conversion results due to the irreversible side reaction of maleimide homo-polymerization. This side reaction becomes apparent at high temperatures for long residence time. However, we found that this side reaction would be significantly mitigated by adding a bit of antioxidants.

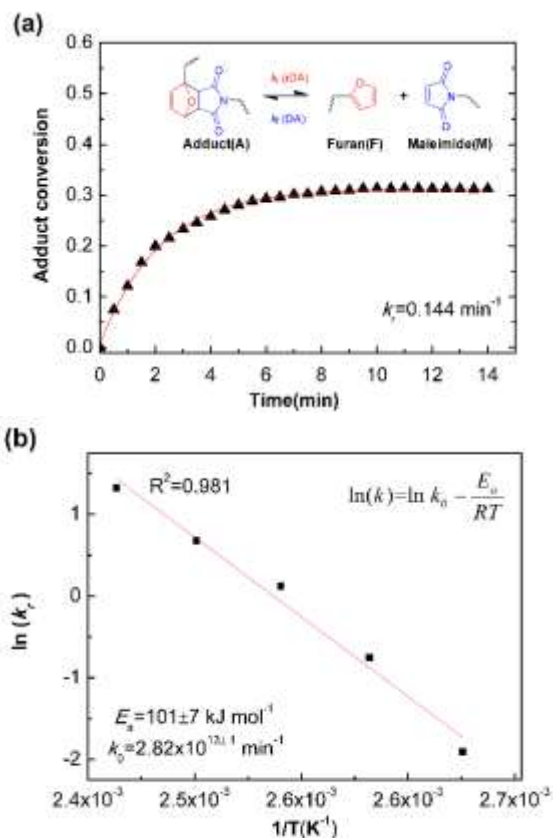


**Fig. 5** (a) Example kinetic parameters for 10F-M at 100 °C. The lines represent fits to eq. 6. Inserted was the Diels-Alder and retro Diels-Alder reactions between furan and maleimide moieties. (b) Arrhenius plot of rDA reaction kinetics for 10F-M sample.

The DA reaction between a maleimide (M) and a furan (F) give an adduct (A), and the rDA reaction proceeds to recover its reactants. A nonlinear least-squares fit of the concentration data by using adduct conversion  $p$  to a kinetic model (eq. 6) was utilized to estimate the reverse rate constants  $k_r$  corresponding to the measurement. More details about the calculation are found in ESI†.

$$\frac{d[A]}{dt} = \frac{d[M]}{dt} = \frac{d[F]}{dt} = k_r[A] - k_f[M][F] \quad (6)$$

Fig. 5a is the evolution of adduct conversion as a function of heating time for 10F-M at 100 °C. The adduct conversion increases sharply within 8 min and levels off at 31% for extended time. The reverse reaction rate constant ( $k_r$ ) was fitted to be  $0.144\text{ min}^{-1}$ , and the corresponding adduct half-life ( $\ln(2)/k_r$ ) is 289 s. The  $k_r$  was determined at 100, 110, 120, 130 and 140 °C (Fig. S4, ESI†). By Arrhenius plot, the pre-exponential factor ( $k_0$ ) and activation energy ( $E_{a,r}$ ) for the rDA reaction were determined to be  $2.82 \times 10^{13\pm 1}\text{ min}^{-1}$

and  $101 \pm 7\text{ kJ mol}^{-1}$ , respectively. The value of  $E_{a,r}$  is higher than the reported results of  $88 \sim 95.2\text{ kJ mol}^{-1}$ .<sup>28, 50</sup> The more difficult diffusion of functional groups between pre-polymer and cross-linker in the solid state reaction should be considered for this result.

The equilibrium temperature-conversion relationship was also revealed by FTIR analysis. The equilibrium constant ( $K_{eq}$ ) is written in terms of the maleimide equilibrium conversion  $p_{eq}$  (eq. 7).

$$K_{eq} = \frac{[A]}{[F][M]} = \frac{1}{[M]_0} \frac{p_{eq}}{(1-p_{eq})(r^{-1}-p_{eq})} \quad (7)$$

As shown in Fig. 6a, the equilibrium conversion of maleimide ( $p_{eq}$ ) in all CANs polymers decreases with the temperature ascension. This result suggests that the formed adducts would gradually reversed into reactants with increasing temperatures. The equilibrium shifting is negligible below 60 °C, but becomes obvious over 80 °C. Meanwhile, the gel point temperatures ( $T_{gel}$ ) can be obtained at  $p_{eq} = p_{gel}$ , which are summarized in Table 3.

Fig. 6b is the Van't Hoff plots, i.e., the natural logarithm of  $K_{eq}$  versus inverse temperature, for CANs polymers. The  $K_{eq}$  increases with decreasing F/M ratios. This is consistent with the general reaction behaviour that adding one of the reactants would drive the equilibrium to products. The enthalpy of reaction ( $\Delta H_r^0$ ) and entropy of reaction ( $\Delta S_r^0$ ) are determined from the slope and intercept of Van't Hoff plots, respectively (Fig. S5, ESI†). The corresponding thermodynamics parameters are summarized in Table 3. The measured  $\Delta H_r^0$  value of  $-55 \sim -71\text{ kJ mol}^{-1}$  is comparable to the reported results of  $-60 \sim -73\text{ kJ mol}^{-1}$ .<sup>28, 41</sup>

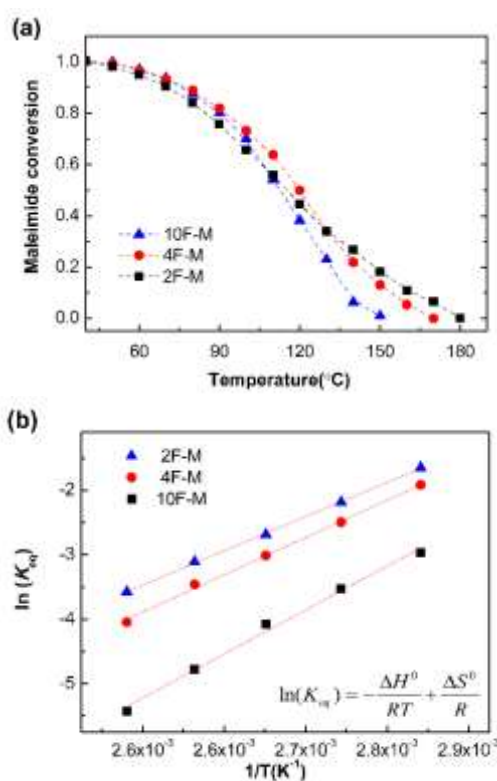


**Fig. 6** (a) The evolution of maleimide equilibrium conversion as the function of temperature for CANs polymers. (b) Van't Hoff plots for CANs polymers with different furan/maleimide ratios. Each

measurement was performed after the reaction equilibrium was obtained.

Sample	$r$	$\rho_{gel}^a$	$T_{gel} (^{\circ}C)^b$	$\Delta H^0 (kJ mol^{-1})$	$\Delta S^0 (J mol^{-1} K^{-1})$
10F-M	1/10	0.29	126	-71±3	-225±9
4F-M	1/4	0.18	143	-60±2	-186±4
2F-M	1/2	0.13	156	-55±1	-170±2

**Table 3** The thermodynamic properties of CANs polymers with different furan/maleimide ratios

<sup>a</sup>  $\rho_{gel}$  was calculated by eq. 3, <sup>b</sup>  $T_{gel}$  is temperature at  $p = \rho_{gel}$ .

### 2.5 Stress relaxation

The time and temperature dependent stress relaxation properties of the CANs polymers were measured by tensile stress relaxation tests. The relaxation time ( $\tau$ ) was determined as the time required to relax to  $1/e$  of the initial modulus.

Fig. 7a depicts the stress relaxation curves of 2F-M sample from 50 °C to 100 °C. The relaxation modulus was normalized and plotted on a double logarithmic scale. Obviously, the modulus decreases at a faster rate when the temperature is higher. For instance, the stress relaxation process is sufficiently increased from 50 °C to 100 °C, as evidenced by  $\tau$  from over  $10^4$  s to 154 s. In addition, cross-linking density has a great effect on the relaxation time of CANs polymers. The CANs elastomers with higher cross-linking densities possess longer relaxation time at the same temperature (Fig. 7b). Therefore, all the chemically cross-linked CANs polymers show relaxation rendered by the dynamic DA/rDA reaction.

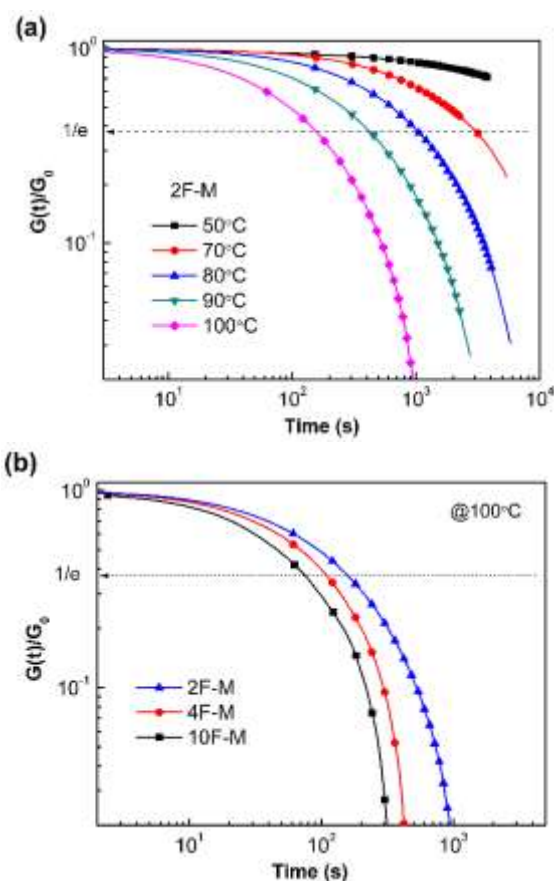


**Fig. 7** (a) Normalized stress relaxation modulus versus time for 2F-M at different temperatures. (b) Normalized stress relaxation modulus versus time for CANs polymers at 100 °C with different F/M ratios.

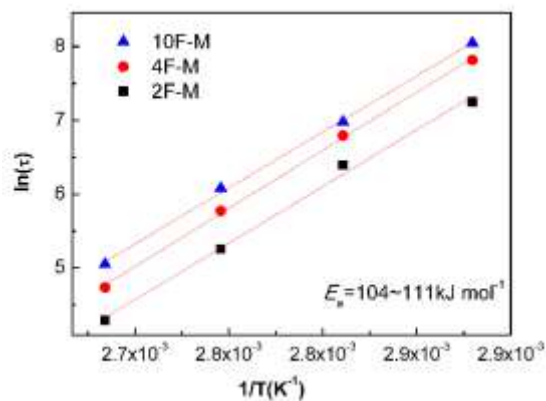


**Fig. 8** Fitting of the relaxation times of CANs polymers to the Arrhenius' equation.

As shown in Fig. 8, the value of  $\tau$  as a function of the inverse temperature follows the Arrhenius' law, which is given by eq. 8:

$$\ln \tau = \ln \tau_0 + \frac{E_a}{RT} \quad (8)$$

The CANs polymers with different F/M ratios showed similar relaxation dynamics characterized by comparable activation energy ( $E_a$ ) of 104 ~ 111 kJ mol<sup>-1</sup>. This value is in the same range of rDA reaction activation energy ( $E_{a,r}$ ) as above mentioned. More details about the relaxation properties can be found (Fig. S6 and Fig. S7, ESI<sup>†</sup>)

Previous study suggests that superposition concept is invalid in

Sample	$p_{gel}$	$T$ (°C)	$p_{eq}$	$\epsilon$	$\ln(\tau)$	$\ln(\tau/\epsilon)$
10F-M	0.29	70	0.94	2.20	7.25	6.46
		80	0.88	1.99	6.39	5.71
		90	0.80	1.74	5.26	4.71
		100	0.70	1.40	4.29	3.95
4F-M	0.18	70	0.93	4.05	7.82	6.43
		80	0.88	3.81	6.79	5.48
		90	0.81	3.43	5.77	4.56
		100	0.72	2.96	4.74	3.68
2F-M	0.13	70	0.91	5.92	8.05	6.65
		80	0.84	5.42	6.98	5.64
		90	0.76	4.79	6.08	4.85
		100	0.66	4.02	5.05	3.96

the DA reaction based reversible network near the gel point.<sup>28</sup> The relaxation tests in our research were performed at the temperatures much lower than  $T_{gel}$ . In addition, the cross-linking density as indicated by the maleimide conversion changes within 25 % in the temperature range of 50~100 °C. Using the stress relaxation time of 10F-M sample at 70 °C as a reference, the shift factor ( $a_T$ ) was calculated for different tests. An approximate linear correlation between the shift factor  $\ln(a_T)$  and inverse temperature was obtained (Fig. S8, ESI<sup>†</sup>). Thus, the temperature-dependent

relaxation for these DA-type CANs well above the gel point can be roughly described by TTS principle. However, the influence of cross-linking density on the relaxation time cannot be interpreted by this phenomenological analysis. A molecular relaxation mechanism should be considered.

Based on the classical gelation theory, Semenov–Rubinstein (SR) theory predicts the relaxation of transient network successfully.<sup>38-39</sup> The characteristic cut-off cluster is the largest “typical” cluster which can achieve complete conformation relaxation.<sup>51</sup> The lifetime of a cluster is defined as the time to break into two parts of comparable size. Above gel point conversion ( $p > p_{gel}$ ) or lower than  $T_{gel}$  ( $T < T_{gel}$ ), the network is formed by the largest cluster with stand size comparable to “typical” cluster. In the CANs polymers well above the gel point, the largest cluster is so large that its conformation cannot relax completely before the break of the “typical” cluster. No matter how far away from the gel point conversion in the post gel region, from the molecular standpoint, the relaxation of such reversible polymer networks is dominated by the lifetime of the “typical” cluster. Hence it is reasonable to expand the SR theory to CANs polymers well above the gel point.

The actual stress relaxation time ( $\tau$ ), comparable to the lifetime of the cut-off cluster, is proportional to the lifetime of adduct ( $\tau_b$ ) and the relative distance to gel point in terms of conversion ( $\epsilon$ ). As  $\tau_b$  is determined by the dynamic chemistry itself, it is expected that the stress relaxation time of CANs polymers with different cross-linking densities can be normalized according to eq. 9:

$$\ln(\tau/\epsilon) - \ln \tau_b = \ln A_0 + \frac{E_{a,r}}{RT} \quad (9)$$

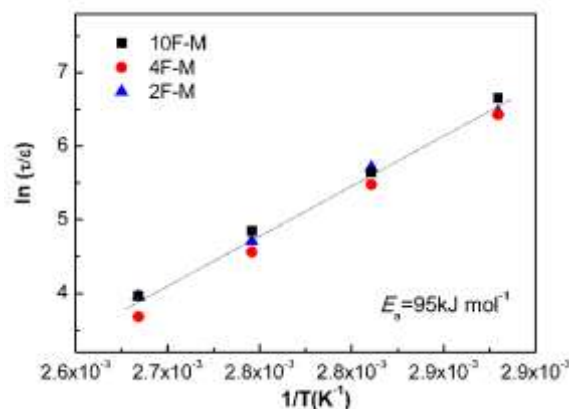


**Fig. 9** Normalized stress relaxation time versus inverse temperature based on eq. 9.

**Table 4** Parameters of stress relaxation dynamics for CANs polymers

Fig. 9 shows that all the measurements located on the same relaxation master curve. As expected, the temperature dependent relaxation can be described by a very simple relationship between the relaxation time and reaction kinetics for DA-type CANs polymers.

As shown in Table 4, the rise in cross-linking densities obviously decreases the value of  $\rho_{gel}$ . The maleimide equilibrium conversion ( $\rho_{eq}$ ) are comparable at the same temperatures among the samples with different F/M ratios, especially at mild temperatures. Consequently, the relative distance to gel point in terms of conversion ( $\epsilon$ ) increases with cross-linking densities. The temperature affects the relaxation time in two aspects. On one hand, higher temperatures lead to shorter bond lifetime ( $\tau_b$ ); on the other hand, increasing the temperature would decrease the cross-linking density contributing to a lower  $\epsilon$ .

The obtained relaxation master curve by SR theory and Arrhenius' equation is dominated by the kinetics of dynamic chemistry instead of the network structure in CANs polymers. The influence of network structure, i.e. cross-linking density, on the temperature-dependent relaxation time can be normalized by the distance parameter  $\epsilon$ . It is noted that half of the activation energy for forward reaction (ca. 20 kJ mol<sup>-1</sup>) is lower than the binding energy of DA adduct (ca. 60 kJ mol<sup>-1</sup>). According to SR theory, the mean time during which the initially DA adduct will find a new partner is the same to the DA bond lifetime.<sup>38</sup> The apparent relaxation activation energy of the master curve is anticipated to be the same to the activation energy of rDA reaction (eq. 9). Thus, this relaxation master curve derived from stress relaxation tests can allow for the determination of reaction kinetics of dynamic chemistry at solid state. Therefore, during the temperature range of  $T_g \sim T_{gel}$ , the SR theory provides a direct relationship between the bond lifetime and the relaxation time for CANs polymers.

From the above results, the mechanism of the DA-type CANs well above gel point was proved to be much similar to that of reversible exchange bond systems. When a DA/rDA reaction equilibrium is approached at a specific temperature, the maleimide conversion or cross-linking density keep constant with time. The relaxation of the DA-type CANs at a relatively mild temperature is determined by the kinetics of dynamic chemistry. The primary distinctions between transesterification-type CANs and DA-type CANs relaxation is the different magnitude of  $\tau_b$  (or  $1/k$ ) and the cross-linking density variation. For instance, the rDA reaction shows a much higher kinetic rate constant (10<sup>0</sup> min<sup>-1</sup>) than the transesterification enhanced by catalysts (10<sup>-4</sup> min<sup>-1</sup>) at 120 °C.<sup>35</sup> The cross-linking density or the relative distance parameter  $\epsilon$  keeps constant for transesterification-type CANs, which decreases with increasing temperature for DA type CANs. Despite of the above differences, the relaxation mechanism for all CANs polymers is due to limited lifetime of dynamic bonds.

This result provide a paradigm to choose the type of dynamic bonds and tune their relaxation behaviour for the rational design of smart materials. For instance, with a relatively weak dynamic bond, increasing the temperature or adding catalyst, a fast local relaxation behaviour can be obtained and an efficient healing is possible. For recyclable thermosets, dynamic bonds with lower lifetime lead to more efficient reprocessing.

### 3 Conclusions

In summary, we have elucidated the relaxation molecular mechanism of CANs polymers well above gel point by a simple scaling relationship between normalized relaxation time and reaction kinetics. In-situ FTIR tests indicate that increasing temperature results in shorter lifetime of dynamic covalent bonds and lower maleimide conversion. The influence of cross-linking density on the temperature-dependent relaxation time can be normalized with the distance from the Flory gel point in terms of conversion. On basis of the Semenov-Rubinstein theory and Arrhenius' law, a simple scaling relationship between normalized relaxation time and reaction kinetics is established. This scaling relationship is anticipated to have wide applicability to both bond exchange and reversible addition reaction type CANs polymers. We believe our result provides a valuable toolkit for better understanding the structure-property relationships of CANs polymers, thus showing new insight into the responsiveness of smart CANs materials at molecular scale.

### Acknowledgements

The authors wish to thank Yanshan Branch, SINOPEC Beijing Research Institute of Chemical Industry for providing the SBR samples.

### Notes and references

- 1 C. J. Kloxin and C. N. Bowman, *Chem. Soc. Rev.* 2013, **42**, 7161.
- 2 C. J. Kloxin, T. F. Scott, B. J. Adzima and C. N. Bowman, *Macromolecules* 2010, **43**, 2643.
- 3 Y. Jin, C. Yu, R. J. Denman and W. Zhang, *Chem. Soc. Rev.* 2013, **42**, 6634.
- 4 X. Chen, M. A. Dam, K. Ono, A. Mal, H. Shen, S. R. Nutt, K. Sheran and F. Wudl, *Science* 2002, **295**, 1698.
- 5 F. Wang, M. Z. Rong and M. Q. Zhang, *J. Mater. Chem.* 2012, **22**, 13076.
- 6 B. Ghosh and M. W. Urban, *Science* 2009, **323**, 1458.
- 7 X. Kuang, G. M. Liu, X. Dong, X. G. Liu, J. J. Xu and D. J. Wang, *J. Polym. Sci., Part A: Polym. Chem.* 2015, **53**, 2094.
- 8 Y. Amamoto, H. Otsuka, A. Takahara and K. Matyjaszewski, *Adv. Mater.* 2012, **24**, 3975.
- 9 Y.-X. Lu and Z. Guan, *J. Am. Chem. Soc.* 2012, **134**, 14226.
- 10 P. Zheng and T. J. McCarthy, *J. Am. Chem. Soc.* 2012, **134**, 2024.
- 11 J. J. Cash, T. Kubo, A. P. Bapat and B. S. Sumerlin, *Macromolecules* 2015, **48**, 2098.
- 12 C. Zeng, H. Seino, J. Ren and N. Yoshie, *ACS Appl. Mater. Interfaces* 2014, **6**, 2753.
- 13 B. T. hermalMichal, C. A. Jaye, E. J. Spencer and S. J. Rowan, *ACS Macro Letters* 2013, **2**, 694.
- 14 Q. Zhao, W. Zou, Y. Luo and T. Xie, *Sci. Adv.* 2016, **2**, e1501297.
- 15 X. Mu, N. Sowan, J. A. Tumbic, C. N. Bowman, P. T. Mather and H. J. Qi, *Soft Matter* 2015, **11**, 2673.
- 16 X. Kuang, G. Liu, X. Dong and D. Wang, *Polymer* 2016, **84**, 1.
- 17 L.-T. T. Nguyen, T. T. Truong, H. T. Nguyen, L. Le, V. Q. Nguyen, T. Van Le and A. T. Luu, *Polym. Chem.* 2015, **6**, 3143.
- 18 Z. Pei, Y. Yang, Q. Chen, E. M. Terentjev, Y. Wei and Y. Ji, *Nat Mater* 2014, **13**, 36.
- 19 Z. Q. Lei, H. P. Xiang, Y. J. Yuan, M. Z. Rong and M. Q. Zhang, *Chem. Mater.* 2014, **26**, 2038.

- 20 R. Long, H. J. Qi and M. L. Dunn, *Soft Matter* 2013, **9**, 4083.
- 21 K. Yu, P. Taynton, W. Zhang, M. Dunn and H. J. Qi, *RSC Adv.* 2014, **4**, 10108.
- 22 X. Kuang, G. Liu, L. Zheng, C. Li and D. Wang, *Polymer* 2015, **65**, 202.
- 23 P. Taynton, K. Yu, R. K. Shoemaker, Y. Jin, H. J. Qi and W. Zhang, *Adv. Mater.* 2014, **26**, 3938.
- 24 O. R. Cromwell, J. Chung and Z. Guan, *J. Am. Chem. Soc.* 2015, **137**, 6492.
- 25 X. Kuang, G. Liu, X. Dong and D. Wang, *Macromol. Mater. Eng.* 2016, **301**, 535.
- 26 B. J. Adzima, H. A. Aguirre, C. J. Kloxin, T. F. Scott and C. N. Bowman, *Macromolecules* 2008, **41**, 9112.
- 27 G. Rivero, L.-T. T. Nguyen, X. K. D. Hillewaere and F. E. Du Prez, *Macromolecules* 2014, **47**, 2010.
- 28 R. J. Sheridan and C. N. Bowman, *Macromolecules* 2012, **45**, 7634.
- 29 A. Gandini, *Prog. Polym. Sci.* 2013, **38**, 1.
- 30 L. L. De Lucca Freitas and R. Stadler, *Macromolecules* 1987, **20**, 2478.
- 31 P. Cordier, F. Tournilhac, C. Soulie-Ziakovic and L. Leibler, *Nature* 2008, **451**, 977.
- 32 W. C. Yount, D. M. Loveless and S. L. Craig, *J. Am. Chem. Soc.* 2005, **127**, 14488.
- 33 L. Imbernon, S. Norvez and L. Leibler, *Macromolecules* 2016, **49**, 2172.
- 34 K. Yu, P. Taynton, W. Zhang, M. L. Dunn and H. J. Qi, *RSC Adv.* 2014, **4**, 48682.
- 35 M. Capelot, M. M. Unterlass, F. Tournilhac and L. Leibler, *ACS Macro Letters* 2012, **1**, 789.
- 36 D. Montarnal, M. Capelot, F. Tournilhac and L. Leibler, *Science* 2011, **334**, 965.
- 37 H. Yang, K. Yu, X. Mu, Y. Wei, Y. Guo and H. J. Qi, *RSC Adv.* 2016, **6**, 22476.
- 38 M. Rubinstein and A. N. Semenov, *Macromolecules* 1998, **31**, 1386.
- 39 A. N. Semenov and M. Rubinstein, *Macromolecules* 1998, **31**, 1373.
- 40 D. Stauffer, *Phys. Rep.* 1979, **54**, 1.
- 41 R. J. Sheridan, B. J. Adzima and C. N. Bowman, *Aust. J. Chem.* 2011, **64**, 1094.
- 42 P. J. Flory, *J. Am. Chem. Soc.* 1941, **63**, 3083.
- 43 L. M. Polgar, M. van Duin, A. A. Broekhuis and F. Picchioni, *Macromolecules* 2015, **48**, 7096.
- 44 E. Passaglia and F. Donati, *Polymer* 2007, **48**, 35.
- 45 C.-D. Varganici, O. Ursache, C. Gaina, V. Gaina, D. Rosu and B. C. Simionescu, *Ind. Eng. Chem. Res.* 2013, **52**, 5287.
- 46 Y. Zhang, A. A. Broekhuis and F. Picchioni, *Macromolecules* 2009, **42**, 1906.
- 47 A. Gandini, D. Coelho and A. J. D. Silvestre, *Eur. Polym. J.* 2008, **44**, 4029.
- 48 J. Canadell, H. Fischer, G. De With and R. A. T. M. van Benthem, *J. Polym. Sci., Part A: Polym. Chem.* 2010, **48**, 3456.
- 49 M. J. He, W. X. Chen and X. X. Dong, *Polymer physics*. 2nd ed.; Fudan University Press: Shanghai, 2000.
- 50 G. Scheltjens, M. M. Diaz, J. Brancart, G. Van Assche and B. Van Mele, *React. Funct. Polym.* 2013, **73**, 413.
- 51 H. J. Herrmann, *Phys. Rep.* 1986, **136**, 153.

